Diffraction of He Atoms at a Si(100) Surface

Mark J. Cardillo and G. E. Becker
Bell Laboratories, Murray Hill, New Jersey 07974
(Received 1 March 1978)

Diffraction of helium atoms at a clear Si(100) surface has been observed. Integral-order, half-order, and quarter-order peaks consistent with the two-domain $c(4\times 2)$ surface reconstruction have been recorded. Additional peaks at the $(\frac{1}{2}\frac{1}{2})$ and $(\frac{3}{2}\frac{3}{2})$ positions are also seen. The diffraction intensities amount to $\sim 10^{-3}$ of the incident beam. The major portion of the scattering is spread over a large range of solid angle with broad maxima characteristic of rainbow scattering.

We have observed the diffraction of thermal-energy He beams from a Si(100) surface. Highly collimated, nearly monoenergetic beams of He strike a Si(100) crystal and the scattered particles are detected by a mass spectrometer rotating in the plane of the beam and surface normal. The incident angle and wavelength (energy) of the beam and the azimuthal orientation of the crystal are varied to confirm the grating relation for all assigned diffraction peaks. Sharp integral and half-order peaks are observed scanning in the $[\bar{1}0]$ direction [see Fig. 1(c)]. Scans in the $[\bar{1}\frac{\bar{1}}{2}]$ direction show quarter-order and half-order peaks confirming that the $c(4\times 2)$ reconstruction observed by low-energy-electron diffraction (LEED)[1] is a property of the outermost surface layer. We have also observed clear $[\frac{\bar{1}}{2}\frac{\bar{1}}{2}]$ and $[\frac{\bar{3}}{2}\frac{\bar{3}}{2}]$ peaks scanning in the $[\bar{1}\bar{1}]$ direction. These features have not been observed in previous LEED studies and their possible origin is discussed below.

Since the first observations of He diffraction from a LiF surface by Estermann and Stern,[2] most studies of atomic diffraction on solid surfaces have focused on ionic materials for which the diffraction intensities are large. In recent years, other surfaces have been shown to diffract light gases. These include W(112),[3] Ag(111),[4] tungsten carbide,[5] and slightly contaminated W,[6] and Cu(117).[7] Diffraction from a semiconductor surface has not been observed previously. A study of He scattering from cleaved Si(111)[8] reported broad scattering distributions with no significant structure. The detailed features we have observed suggest that molecular beam scattering may indeed provide significant structural information complementary to LEED in the study of reconstructed semiconductor surfaces.

The apparatus has been described elsewhere[9] and we note here only the pertinent features. A beam source produces a He jet from a high-pressure expansion with a narrow velocity distribution (full width at half-maximum $\sim 0.12 v_{mp}$) over a range of energies. The beam may be accelerated by heating the nozzle source and decelerated by mixing the He with Ar. The energies (wavelength) for these experiments are in the range 0.018 eV ($\lambda = 1.06$ Å) $\leq E \leq 0.20$ eV ($\lambda = 0.32$ Å). The crystal is mounted in a uhv chamber ($P \sim 6\times 10^{-10}$ Torr) which also contains a cylindrical-mirror-analyzer Auger spectrometer (AES) and separate LEED optics. The mass spectrometer can rotate about the crystal axis up to 200° and detects the density of scattered He with $\sim 1.4°$ resolution. It is enclosed by a differential pumping can in which the pressure is generally less than 2×10^{-10} Torr. For these experiments, the incident He beam is square-wave modulated and collimated to 0.06°. The scattered He signal is fed to a lockin ampli-

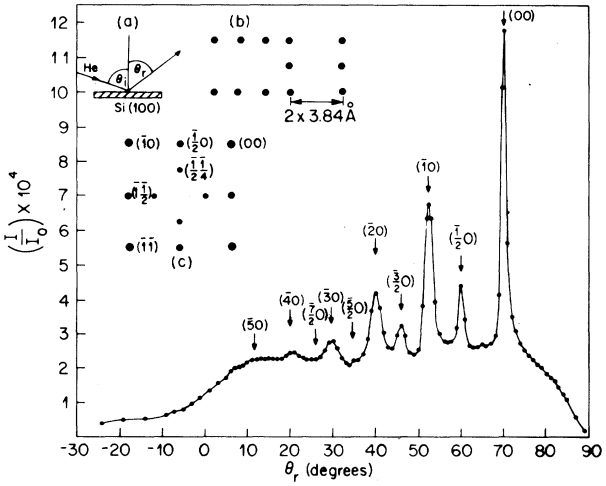

FIG. 1. He intensity normalized to the incident beam as a function of scattering angle. The angular positions marked with arrows were calculated from the grating formula $n\lambda = d(\sin\theta_r - \sin\theta_i)$ with $\theta_i = 70°$, $\lambda = 0.57$ Å, $d = 3.84$ Å. Inset (a) shows the scattering geometry, (b) the real-space periodicity for a two-domain 2×1 net for Si(100), (c) a schematic LEED diffraction pattern expected for a two-domain Si(100) $c(4\times 2)$ surface with selected spots indexed.

fier.

The crystal was cut and polished outside the vacuum chamber and cleaned *in situ* by room-temperature ion bombardment followed by 5–10 min of annealing at 850°C. After this preparation we see a sharp reproducible 2×1 two-domain LEED pattern (Fig. 1) and an AES spectrum with carbon as the sole residual impurity with a ratio of peak-to-peak signals of C at 272 eV and Si at 92 eV of $\lesssim 0.005$. At grazing incident angles ($\theta_i = 70°$) the specular intensity decreases noticeably in minutes due to the adsorption of small fractions of a monolayer of residual gases at 6×10^{-10} Torr. Consequently, during the runs, the crystal is flashed to 850°C for approximately 1 minute every 20 minutes. This procedure completely restores the specular intensity. During a run the mass spectrometer is advanced in steps of 1° or 2° with a precision of 0.2°. The incident angle, θ_i, is determined to ~0.3°. The relative azimuthal angle is set to ~1° but the absolute azimuthal orientation of the crystal is known to ~3°.

In Fig. 1 we display the results of a scan where the scattered beam projects onto the [10] direction of the surface unit mesh. The insets show the scattering geometry, the surface real-space net corresponding to two domains of 2×1 reconstruction, and a schematic LEED pattern expected for the two-domain 2×1 reconstruction with additional two-domain centered quarter-order spots. This latter feature is believed to be characteristic of a clean well-ordered Si(100) surface.[1,10] Our sample is apparently not ordered well enough to permit observation of quarter-order beams with LEED. Several features of the data should be noted. The diffracted intensities are only 10^{-3}–10^{-4} of the incident beam. The balance of the scattering is phase incoherent and/or inelastic and constitutes a relatively smooth background on top of which the diffraction peaks sit. This smooth background appears to be cut off around normal emission ($\theta_r \sim 0°$). We note that the solid angle subtended by the detector is of the order of 10^{-4} sr. Thus, if nearly all the signal is due to diffuse scattering it can easily be of the order of $I/I_0 \sim 10^{-4}$. The spatial focusing of the diffraction peaks allows them to be detected. In these experiments the wavelength spread due to the incident He velocity distribution and the angular resolution of the detector account for the width of the diffraction peaks.

The $(\frac{1}{2}0)$ and $(\frac{3}{2}0)$ peaks in Fig. 1 are about half the intensity of the $(\bar{1}0)$ and $(\bar{2}0)$ peaks, respectively. Since only half the illuminated region of the crystal contributes to the half-order peaks, the surface perturbation giving rise to the half-order peaks is comparable in scattering strength to that of the rows with periodicity of the unreconstructed net which contribute only to the integral-order peaks. This indicates that the perturbation of the outermost surface layer giving rise to the doubled periodicity is a major distortion.

In Fig. 2 we plot the scattered intensity projecting along the [10] azimuth for $\theta_i = 70°$ at three He wavelengths. The abscissa is proportional to $|\Delta\vec{k}_{\parallel}| = \vec{k}_{i\parallel} - \vec{k}_{r\parallel}$ where $\vec{k}_{i\parallel}$ is the projection of the incident wave vector onto the surface, $(2\pi/\lambda) \times \sin\theta_i$, and the subscript r denotes the reflected wavevector. For surface diffraction a reciprocal net vector $|\vec{G}| = 2\pi n/d$ equals the He momentum transfer parallel to the surface; i.e., $|\vec{k}_{i\parallel} - \vec{k}_{r\parallel}| = (2\pi/\lambda)(\sin\theta_i - \sin\theta_r)$. Thus in Fig. 2 all the diffraction features should occur at the same values

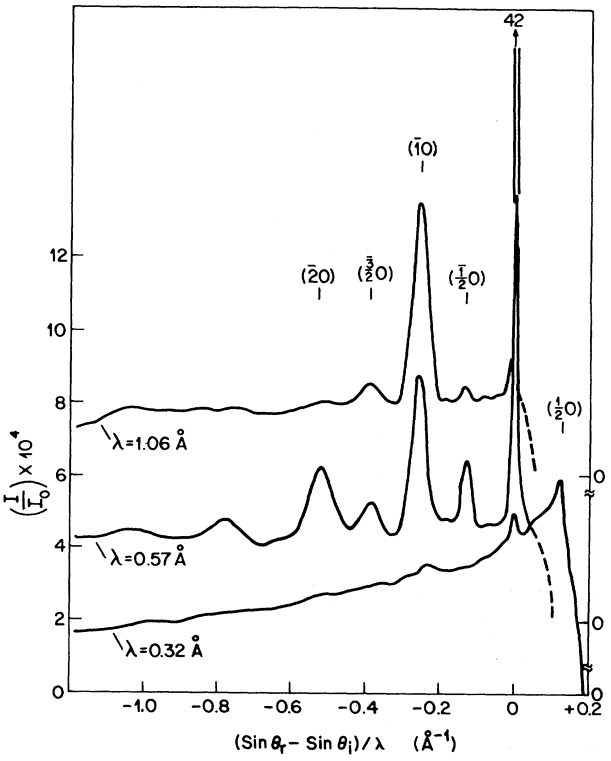

FIG. 2. Normalized scattered helium intensity for $\theta_i = 70°$ as a function of $(\sin\theta_r - \sin\theta_i)/\lambda$, proportional to the change in momentum parallel to the surface, for three helium energies (or wavelengths). The Bragg condition requires that peaks of the same order, n, be vertically aligned. For clarity, the curves have been displaced vertically.

of $\Delta\vec{k}_{\parallel}$. We note the vertical alignment of features at integer multiples of the value 0.13 which yields a spacing of 7.68 Å as expected for the doubled periodicity. At $\lambda = 0.32$ Å the diffraction peaks are small. The background scattering is dominant and reaches a maximum beyond the specular angle near grazing exit. At $\lambda = 1.06$ Å the background is nearly uniform in angle. As the incident energy and background scattering decrease and the wavelength increases, the diffraction intensities are generally expected to increase. However, at $\lambda = 1.06$ Å the half-order diffraction features are considerably smaller than at $\lambda = 0.57$ Å whereas the $(\bar{1}0)$ and specular peaks are larger. This may be due in part to the large lateral coherence of the incident beam (10^2–10^3 Å) whereby many orthogonal domains contribute to each scattering event. It is likely that these domains are separated by steps with terraces significantly displaced vertically (1.3 Å) compared to the He wavelength. This would lead to interference effects from multidomain coherent scattering, affecting the specular as well as the diffracted peaks. In addition to coherent interference, bound-state resonances can strongly modulate the specular and diffraction intensities. A study of these effects will require a fine grid of data.

In Fig. 3 we plot the scattering results for three angles of incidence, $\theta_i = 30°$, 50°, and 70°. The expected positions of the integral- and half-order diffraction peaks are indicated. As the incident beam moves toward the crystal normal the diffracted intensities decrease. Note that the broad structure in the background scattering changes significantly with incident angle. For example at $\theta_i = 50°$ there is a large hump at $\theta_r = -10°$. At $\theta_r = +10°$ there is a similar feature on top of which the $(\bar{3}0)$, $(\frac{\bar{7}}{2}0)$, and $(\bar{4}0)$ diffraction peaks may be seen. We believe these features are rainbow maxima which have been observed in atom surface scattering several times previously.[11] They are a result of points of inflection in a periodic potential. It is possible to obtain complementary structural information from these background features. If the major part of the background scattering is due to collisions with small energy transfer (i.e., bulk phonon excitations), one expects that the differential cross section is similar to that for elastic scattering but with a loss of coherence (diffraction). Thus classical "elastic" scattering considerations may be appropriate for analysis of this background. In particular, with simple model potentials and topographical analysis one may infer the potential contours of the unit mesh from the energy and angle dependence of the rainbow maxima and cutoffs.[12]

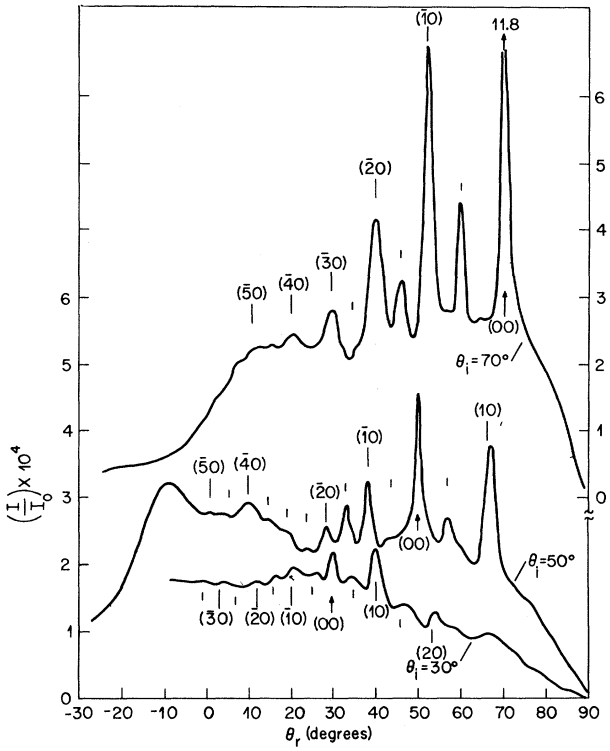

FIG. 3. Normalized scattered helium intensity ($\lambda_{He} = 0.57$ Å) as a function of scattering angle for three angles of incidence θ_i. For clarity, the curve for $\theta_i = 70°$ has been displaced upwards. The expected positions for surface diffraction are indicated and the integral-order reflections labeled.

Finally, we note that for scans in the $[\bar{1}\frac{\bar{1}}{2}]$ direction we observe a broad $(\frac{\bar{1}}{2}\frac{\bar{1}}{4})$ weak diffraction peak and the higher-order peaks expected for the $c(4\times2)$ two-domain reconstruction of the Si surface. Furthermore, we observe in the $[\bar{1}\bar{1}]$ direction $(\frac{\bar{1}}{2}\frac{\bar{1}}{2})$ and $(\frac{\bar{3}}{2}\frac{\bar{3}}{2})$ peaks as well as the $(\bar{1}\bar{1})$ and $(\bar{2}\bar{2})$ peaks. The $(\frac{\bar{1}}{2}\frac{\bar{1}}{2})$ is the most intense $[I(\frac{\bar{1}}{2}\frac{\bar{1}}{2})/I_0 \sim 1\times10^{-4}]$ along that projection. Note that at the $(\frac{\bar{1}}{2}\frac{\bar{1}}{2})$ position in Fig. 1(c) there is no diffraction expected. However, in the original observation of the quarter-order reconstruction[1] the diffraction spots appear streaked. Our scans in directions between the $[\bar{1}\frac{\bar{1}}{2}]$ and $[\bar{1}\bar{1}]$ directions indicate the quarter-order diffraction features are streaked as well. The overlap of four quarter-order features streaked to the center of each reciprocal mesh may result in a substantial intensity peak at the $[\frac{\bar{1}}{2}\frac{\bar{1}}{2}]$ position. Another explanation of intensity at the $(\frac{\bar{1}}{2}\frac{\bar{1}}{2})$ position may be coherent diffraction from several orthogonal do-

mains lying within the coherence area of the incident beam. Multidomain diffraction effects are not well studied but are likely to occur in these experiments.[13]

We also observe small additional bumps along each direction between the diffraction peaks attributable to the $c(4\times2)$ pattern. To our knowledge, they have not been reported previously, but Sakurai and Hagstrum have recently photographed a LEED pattern for Si(100) with weak extra spots similarly positioned.[14]

In summary, we have observed extensive diffraction of a He beam by a Si(100) surface. The scattering pattern consists of integral-order, half-order, and weak quarter-order diffraction peaks indicating that the surface is reconstructed to a two-domain $c(4\times2)$ structure. The reconstruction giving rise to the quarter-order features is sufficiently weak that we do not see it with our LEED optics. He scattering is apparently more sensitive to weak surface structural perturbations. Diffraction peaks are seen at the $(\frac{1}{2}\frac{1}{2})$ and $(\frac{3}{2}\frac{3}{2})$ positions whose origin is not yet clear. The diffracted intensity constitutes $\sim 10^{-3}$ of the total scattered intensity. The major portion of scattered He appears as a smooth background extending over a large range of solid angle and shows broad structural features suggestive of complex rainbow scattering.

We thank J. Appelbaum, E. G. McRae, and J. E. Rowe for stimulating discussions and E. E. Chaban for technical assistance.

[1]J. J. Lander and J. Morrison, J. Chem. Phys. 37, 729 (1962).
[2]I. Estermann and O. Stern, Z. Phys. 61, 95 (1930).
[3]D. V. Tendulkar and R. E. Stickney, Surf. Sci. 27, 516 (1971).
[4]G. Boato, P. Cantini, and R. Tartarek, J. Phys. F 6, 2237 (1976).
[5]W. H. Weinberg and R. P. Merrill, Phys. Rev. Lett. 25, 118 (1970).
[6]J. Horne and D. R. Miller, J. Vac. Sci. Technol. 13, 351 (1976).
[7]J. Lapujoulade and Y. Lejay, Surf. Sci. 69, 354 (1977).
[8]D. E. Houston and D. R. Frankl, J. Chem. Phys. 60, 3268 (1974).
[9]M. J. Cardillo, C. S. Y. Ching, E. F. Greene, and G. E. Becker, to be published.
[10]M. B. Webb (private communication) reports sharp but weak quarter-order structure (3% of integral-order spot intensity) for high-temperature–annealed Si(100) $c(2\times4)$ observed with a Faraday cup.
[11]F. O. Goodman, Crit. Rev. Solid State Sci. 7, 33 (1977).
[12]E. F. Greene and E. A. Mason, to be published.
[13]G. J. Russell, Surf. Sci. 19, 217 (1970) reported a high-energy-electron diffraction pattern (HEED) of Ge(100) $c(4\times2)$ with spots at the $[\frac{1}{2}\frac{1}{2}]$ positions which he did not observe in LEED. The lateral coherence in HEED is in general significantly greater than in LEED.
[14]T. Sakurai and H. D. Hagstrum, private communication. Here the quarter-order features are also sharp as in Ref. 10.

Landau-Level–Electron Lifetimes in *n*-InSb

E. Gornik,[a] T. Y. Chang, T. J. Bridges, V. T. Nguyen, and J. D. McGee
Bell Telephone Laboratories, Holmdel, New Jersey 07733

and

W. Müller
Institut für Physikalische Elektronik, Technische Universität Wien, Austria, and Ludwig Bolzmann–Institut für Festkörperphysik, Wien, Austria

(Received 21 November 1977)

Saturation measurements of magnetoabsorption in n-InSb have shown that electron-electron scattering determines the electronic lifetime in the first Landau level, giving values of $\sim 10^{-10}$ sec for excited electronic densities of 10^{13} cm^{-3}. Lifetimes in impurity levels are $\sim 10^{-7}$ sec determined by acoustic phonon scattering.

In this Letter we report the first measurement of intraband electron lifetimes ($T_{1,+}$) in the first Landau level of a narrow-gap semiconductor—in the present case InSb. The observed lifetimes ($T_{1,+}\sim 10^{-10}$ sec) are consistent with electron-electron scattering as the dominant relaxation process and the inverse linear dependence of T_{1+} on electron concentration confirms this mecha-

